Cavity-enhanced detection of surface photovaporization

E. C. Benck, Z. Rong, S. H. Chen, Z. C. Tang, and H. A. Schuessler
Department of Physics, Texas A&M University, College Station, Texas 77843

(Received 3 August 1990; accepted for publication 4 February 1991)

Cavity-enhanced detection is used to monitor minute vapor plumes produced by focusing a pulsed laser beam onto a surface placed inside a resonant optical cavity. The photovaporization signals from a variety of different materials are examined, with emphasis being placed on their amplitude and temporal structure.

Cavity-enhanced detection[1–3] can be used as a sensitive means of monitoring laser-surface interactions. In particular, it can detect the amount of material ejected from a solid- or liquid-film surface when a laser beam is focused onto it. The tiny ablation plume is monitored inside an optical cavity by a fixed frequency continuous-wave (cw) probe beam. The photovaporization signal is produced by changes in the optical path length, absorption, and scattering of the probe beam by the laser-ablation plume. The signal is amplified by the quality factor of the high finesse optical cavity, since the probe beam frequency is resonant with a cavity mode. The new technique can be used to monitor and control (via feedback) laser etching, micromachining, and annealing of surface films. In addition, delicate surfaces can be cleaned of particulate and micron-sized contaminants.

In this letter we report details of laser-ablation plume formation for a variety of refractory and low melting point materials. The absorption of a tightly focused pulsed laser beam on a surface creates localized surface heating. This localized heating results in both melting and vaporizing. Thermal surface effects have been previously modeled[4] for the case of steady-state material removal. The calculation is based on the assumptions of one-dimensional fluid flow of the molten material on the surface and of an optically thin vapor plume. Extrapolation of the calculations to pulsed laser ablation indicates that liquid expulsion from the surface can be greater than the vaporization losses, even at the low laser powers used in the present study.

Figure 1 depicts the experimental apparatus. The vaporization is produced by a tunable pulsed dye laser which is focused onto the sample located inside a spherical etalon. The pulsed dye laser produces pulse energies in the range of 0.35–35 μJ at $\lambda = 640$ nm with a pulse width of 10 ns. When focused to a spot size of 20 μm, this corresponds to an intensity of 0.1–11 W/μm^2. The material removed from the surface is monitored by a weak HeNe-laser probe beam. In the present experiment, a mode-matched HeNe beam is split into two beams, and both are injected into the etalon. One beam is used as the probe beam and grazes the sample surface above the focal spot of the pulsed dye laser beam. The other beam is used to stabilize the étalon by locking it to the side of a transmission fringe and, thereby, to the HeNe-laser frequency.

In all our measurements the focused laser spot size was kept the same. Using for size reference a calibrated Ronchi grating as the target, the spot size was measured to have a diameter on the surface of 20 μm. The photovaporization signal as a function of position on the Ronchi grating is shown in Fig. 2.

More than 25 different materials were examined to investigate the various vaporization signals. Where possible, the samples were polished with a fine grit and occasionally were also acid etched. The most interesting features were obtained from metals and opaque films. Three features, namely, the magnitude of the vaporization amplitude, the temporal evolution of the plume, and the velocity of the ejected material were studied in detail. The results are compiled in Table I. The strongest photovaporization signals were obtained from aluminum surfaces which had an 80% peak attenuation of the probe beam. The weakest signal occurred for tungsten, which produced a 1.5% peak attenuation. Transparent materials, such as glass and Plexiglas, and highly reflective materials, such as Teflon and Spectralon, did not produce any observable signals at the present low laser powers.

The most common temporal structure observed in the vaporization signals consisted of a single asymmetric peak, as shown for aluminum in Fig. 3. It has a rise time of about 0.5 ms and a much slower decay time of about 14 ms. For some samples, a second broad peak, centered about 2 ms after the laser pulse, occurred in the averaged data, as is shown for lead in Fig. 3. This broadened peak displayed considerable variations in shape when observed on a shot-to-shot basis. For the dye laser pulses with the highest

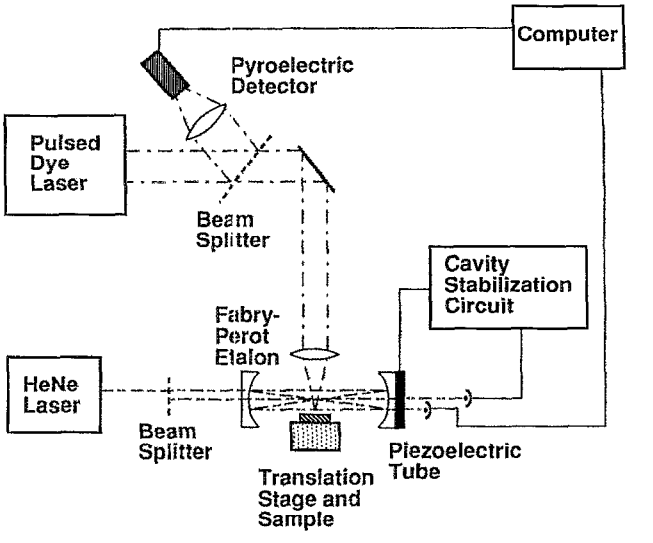

FIG. 1. Schematic diagram of the experimental apparatus.

 0003-6951/91/141476-03$02.00

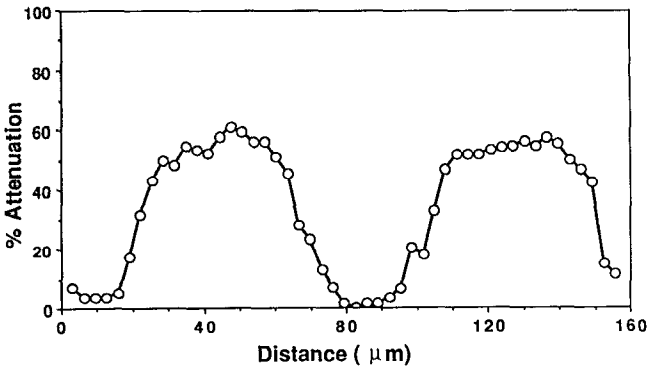

FIG. 2. Photovaporization signals from aluminum and lead. The pulsed dye laser was operating with a power of 35 μJ per pulse. The curves are the averaged result of the signals from 50 laser pulses.

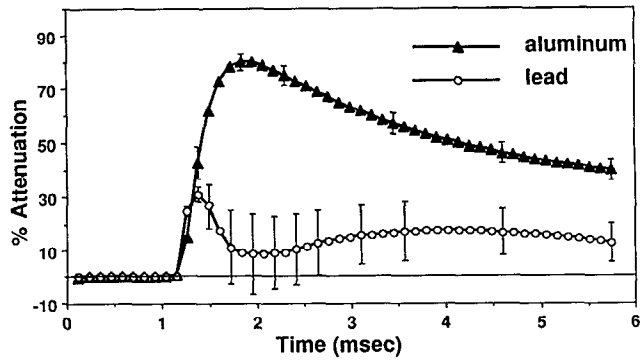

FIG. 3. Photovaporization signal vs position on a Ronchi grating. Each data point respresents the peak signal from a single laser pulse with an energy of 15 μJ. The period of the grating is 80 μm.

energy of 35 μJ, this second peak was present in all samples with melting points less than 400 °C. As the laser intensity was reduced, the second peak disappeared leaving only the normal single peak behavior. It is assumed that this second peak arises due to the localized melting of the surface which becomes deep enough to develop turbulent convection and even boiling.

The second peak can also arise from the vaporization of a second species which has a higher activation energy than the first one. The actual surface modifications were also studied using both a light and a scanning electron microscope (SEM), as shown in Fig. 4. They varied considerably depending on the material. The width of the surface modification, produced on low melting point targets, such as lead (T_m = 327 °C), is three times larger than the focal spot of the laser. In the other extreme, the cratering produced in refractory metals, such as tungsten (T_m = 3410 °C), is much smaller than the focal spot and has a diameter of only a few μm. For thin films, such as aluminum on glass, the film could be completely removed, leaving essentially a clean substrate.

The average velocity of particles leaving the surface was also investigated. For this measurement, the time delay between the dye laser pulse and the start of the photovaporization signal as a function of the probe beam's height above the surface was observed. When the probe beam grazed the surface, the signal occurred instanta-

TABLE I. Compilation of the maximum height of the photovaporization signals for different materials. A pulsed dye laser beam focused to a diameter of 20 μm with an energy of 35 μm and 10 ns pulse duration produced the ablation plume. For the materials which displayed two maxima (melting point < 400 °C), the height of the first and second peaks are listed.

Material	Signal height (% change) First peak	Second peak	Melting point (°C)
mercury	43 (13)	34 (11)	− 39
indium	44 (3)	67 (7)	157
tin	59 (4)	72 (7)	232
bismuth	34 (10)	41 (19)	271
cadmium	49 (16)	37 (25)	321
lead	33 (3)	18 (10)	328
aluminum	80 (3)		660
silver	33 (10)		962
gold	3.4 (2.5)		1064
copper	12 (2)		1083
silicon	27 (15)		1410
stainless steel	34 (7)		1427
nickel	48 (6)		1453
palladium	54 (4)		1552
platinum	5.6 (2)		1772
molybdenum	22 (4)		2617
tantalum	no signal		2996
carbon (graphite)	53 (11)		~3350
tungsten	1.5 (0.6)		3410

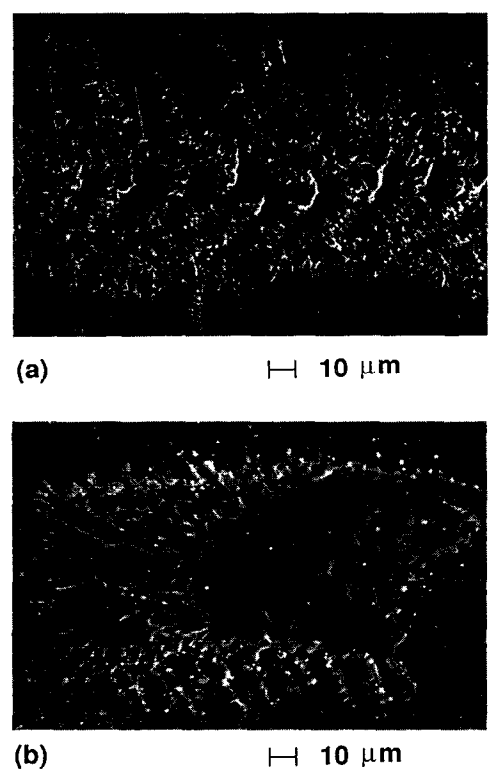

FIG. 4. Scanning electron micrographs of the surface traces due to the pulsed laser irradiation of (a) palladium and (b) bismuth.

neously, and for larger heights a time delay occurred. For aluminum and lead, signals could be obtained up to heights of 1.5 and 6.5 mm, respectively. The corresponding velocities of the ejected materials were 2 m/s and 9 m/s, respectively, for these two metals. This is significantly slower than predicted for photovaporization in vacuum and indicates the effects of the viscous drag forces in air, which slow down the particles in the present experiment.

The contribution to the photovaporization signal resulting from changes in the optical path length can be differentiated from those due to absorption and scattering by locking the cavity to different sides of the transmission fringe of the unperturbed locking HeNe-laser beam. On one hand, optical path length changes of the probe HeNe-laser beam cause a shift in the probe beam fringe so that the photovaporization signal is proportional to the slope at the locking point. The photovaporization effect produces then either a positive signal (when locked to the right side) or a negative signal (when locked to the left side). On the other hand, absorption and scattering contributions are losses and reduce only the photothermal signal amplitude and are as such independent of the locking point. The high sensitivity of the present experiment allowed the observation of minute laser plumes. For such a case, the magnitude of the positive and negative signal is the same, and the signal is entirely caused by optical pathlength changes.

In summary, cavity-enhanced detection is an ultrasensitive technique for monitoring the density and time evolution of minute photovaporization plumes, which are too weak to be visible by the naked eye and which are also in the few ten micron size range in lateral extent.

This work was supported by the Texas Advanced Research Program, NSF, and the Center for Energy and Mineral Resources at Texas A&M University.

[1] Q. Yu, S. H. Chen, Z. Rong, Y. Xu, and H. A. Schuessler, Chin. J. Laser **16**, 87 (1989).
[2] S. H. Chen, Z. C. Tang, Z. Rong, and H. A. Schuessler, SPIE Proc. **1208**, 149 (1990).
[3] S. H. Chen, Z. C. Tang, Z. Rong, and H. A. Schuessler, SPIE Proc. **1302**, 187 (1990).
[4] C. L. Chan and J. Mazumder, J. Appl. Phys. **62**, 4579 (1987).